PHILOSOPHICAL TRANSACTIONS OF THE ROYAL SOCIETY A MATHEMATICAL, PHYSICAL & ENGINEERING SCIENCES

Modelling deformation microstructure with the crystal plasticity finite –element method

Peter Bate

Phil. Trans. R. Soc. Lond. A 1999 **357**, 1589-1601
doi: 10.1098/rsta.1999.0391

THE ROYAL SOCIETY

Modelling deformation microstructure with the crystal plasticity finite-element method

By Peter Bate†

IRC in Materials for High Performance Applications and School of Metallurgy and Materials, The University of Birmingham, Birmingham B15 2TT, UK

The finite-element (FE) method is commonly used to solve boundary-value problems in continua. Constitutive equations based on crystal plasticity have been implemented in FE simulations, and these slip-based calculations have the potential to model a variety of interesting phenomena. However, the substructure of the deformed state in metals is inherently discontinuous. To what extent continuum plasticity calculations can be reasonably used for deformation microstructure predictions depends on the microstructural interpretation of the constitutive models. It is possible with quite simple models to predict orientation gradients at large second-phase particles and at grain boundaries. Because of the implicit link between the substructure and mechanical behaviour of metals, and the great flexibility that crystal plasticity models have, the prediction of at least some of the more important aspects of substructure, by association with state variables, is possible.

Keywords: continuum approximation; rate-sensitive slip; orientation splitting; deformation banding; relaxed constraint; recrystallization modelling

1. Introduction

The use of continuum methods for microscale problems is attractive, but is also fraught with difficulties. For modelling deformation substructure, we do not need to consider atoms but generally need to consider dislocations. There are relationships between the behaviour of large numbers of dislocations and continuum approximations: Eshelby (1958) knew this, and also the tendency for 'the physicist to cling to the continuum point of view as long as he can'. That tendency is weakening, and discrete dislocation solutions (van der Giessen & Needleman 1995) are becoming more popular as computers improve. However, it is probably beyond current technology to apply such methods to a 1 mm^3 volume of, say, deformed aluminium and at that scale some kind of continuum method must currently be applied to simulate what the material effectively solves with 10^{20} simple parallel processors. The finite-element method, using constitutive models based on crystal plasticity (crystal plasticity finite-element method (CPFEM)) is potentially useful in this respect.

This method has been in use and development, particularly in the USA, for many years now. It became known to the metallurgical community via the work of Peirce *et al*. (1982, 1983). Since then, there has been much work aimed at either using this method to predict plastic anisotropy, or, more significantly, the development of crystallographic texture. The method has been used in a form where each material (integration) point is the agglomeration of a number of orientations—typically

† Present address: DONCASTERS plc, 28–30 Derby Road, Melbourne, Derbyshire DE73 1FE, UK.

a few hundred—each deforming identically, for example in the work of Kalidindi *et al*. (1992). This, then, essentially invokes the Taylor assumption, but it is deviations from that idealization which are most interesting. Introducing discretization at less than or equal to the grain scale allows simulation of the effects of intergranular mechanical inhomogeneity, and the work of Sarma & Dawson (1996*a*) and Dawson & Marin (1997) has shown that this has very significant effects on deformation texture development which would be extremely difficult to take into account using simpler models. The work presented here explores the application of the CPFEM to predicting intragranular deformation microstructures. By discretizing at the subgrain scale we are, following Eshelby's observation, pushing the continuum approach to, or perhaps beyond, its limit and it remains to be seen how useful the approach is at such length-scales.

Crystal plasticity leads to equations which are difficult to solve. Ideal plasticity, without rate sensitivity, leads to singularities: vertices on yield surfaces and often an indeterminacy in slip system selection. The well-known Taylor and Bishop and Hill models are not in a form which is easily assimilated into finite-element (FE) calculations, and the usual way of overcoming this problem is to invoke rate sensitivity of the slip. This 'rounds off' the step function in the slip response to resolved shear stress. However, for most cases the rate sensitivity needs to be small and, although the resulting equations are now solvable in principle, they present considerable problems in practice.

2. A formalism for finite-element implementation of crystal plasticity

A further problem with the FE implementation of crystal plasticity is the need for finite deformation increments. As long as the finite increments are reasonably small, of the order of 1% or less, then an additive decomposition of strain into elastic and plastic parts can be assumed and, conveniently, backward Euler integration used. That essentially means that equilibrium is determined at the end of each time-step, and that strain and rotation increments are given simply by the terminal strain rate and spin multiplied by that time-step. This formalism is implicit and of course nonlinear, and the solution method used here requires three levels of iteration. The first level is the determination of slip increments from a trial stress state. That stress state in turn is determined from the overall strain increment, and the top level of iteration solves the overall state of quasi-static equilibrium in the domain.

The first two levels of iteration are carried out at each integration point of the FE mesh. The slip stresses $\boldsymbol{\tau}$ are given by the following expression in terms of the (plastic) slip strain increments, $\Delta\boldsymbol{\gamma}$:

$$\tau_\alpha = \tau_\alpha^0(\Delta\gamma_\beta)\left(\frac{\Delta\gamma_\alpha}{\Delta t}\right)^m, \tag{2.1}$$

where $\boldsymbol{\tau}^0$ are slip resistances, Δt is the time-step and m is the slip-rate sensitivity. Indices in Greek text refer to slip system numbers, 1 to 12 here, and those in Roman to spatial coordinates, 1 to 3. The solution of equation (2.1) for the slip increments is not a simple matter. Generally, the slip rate sensitivity is small, say 0.01, and the strain hardening matrix,

$$H_{\alpha\beta} = \frac{\partial\tau_\alpha^0}{\partial\Delta\gamma_\beta}, \tag{2.2}$$

is often nearly singular. In this situation it is convenient to take the logarithmic form of equation (2.1),

$$\ln \tau_\alpha = \ln \tau_\alpha^0(\Delta\gamma_\beta) + m(\ln \Delta\gamma_\alpha - \ln \Delta t), \tag{2.3}$$

and solve using the iteration

$$\Delta\gamma_\alpha^+ = \Delta\gamma_\alpha \exp\left\{ \left[\frac{\Delta\gamma_\beta}{\tau_\alpha^0} H_{\alpha\beta} + m\delta_{\alpha\beta} \right]^{-1} (\ln \tau_\beta - \ln \tau_\beta^0(\Delta\gamma_\rho) - m(\ln \Delta\gamma_\beta - \ln \Delta t) \right\}. \tag{2.4}$$

This is possible because a reasonable initial guess (predictor) for $\Delta\gamma_\alpha$ will give the correct *signs* for the slips, provided some very simple conditions are met. That predictor is based on the formula,

$$\Delta\gamma_\beta = \Delta t \left\{ \frac{\tau_\alpha}{\tau_\alpha^0(\phi)} \right\}^{1/m}, \tag{2.5}$$

where $\tau_\alpha^0(\phi)$ is based on the last estimate obtained for the slips, and this predictor is applied with every new estimate of stress to avoid prejudicing the operative slip systems. This iteration has worked quite well. The predictor allows the definition of 'active' systems, which facilitates size reduction of the various linear equation systems; very desirable for efficient computation. The requirement of a good predictor estimate constrains increment sizes, and the initial values need to be capped.

Given the slip magnitudes for a given stress, it is necessary to iterate for the stress, $\boldsymbol{\sigma}$, given the overall estimate of strain increment, $\Delta\boldsymbol{\varepsilon}$, which is a sum of elastic and plastic components. The iteration used is

$$\sigma_{ij}^+ = \sigma_{ij} + [s_{ijkl} + m_{ij}^\alpha m_{kl}^\beta X_{\alpha\beta}^{-1}]^{-1} \{\Delta\varepsilon_{kl} - s_{klmn}\Delta\sigma_{mn} - m_{kl}^\rho \Delta\gamma_\rho\}, \tag{2.6}$$

where $\boldsymbol{s}$ is the elastic compliance, $\Delta\boldsymbol{\sigma}$ is the Cauchy stress increment in the current coordinate system, $\boldsymbol{X}$ is the visco-plastic hardening matrix,

$$X_{\alpha\beta} = \delta_{\alpha\beta} m \frac{\tau_\alpha}{\Delta\gamma_\alpha} + \frac{\tau_\alpha}{\tau_\alpha^0} H_{\alpha\beta}, \tag{2.7}$$

and $\boldsymbol{m}$ is the Schmid matrix:

$$m_{ij}^\alpha = \tfrac{1}{2}\{b_i n_j + b_j n_i\}_\alpha. \tag{2.8}$$

The Schmid matrix relates the slip stress and strain to the overall stress and plastic strain increment by

$$\tau_\alpha = m_{ij}^\alpha \sigma_{ij}, \qquad \Delta\varepsilon^{p_{ij}} = m_{ij}^\alpha \Delta\gamma_\alpha, \tag{2.9}$$

where $\boldsymbol{b}^\alpha$ and $\boldsymbol{n}^\alpha$ are the cosines of the directions and planes of system α in the current spatial frame.

Solution for overall equilibrium follows the usual implicit FE formalism for elasto-plastic problems. The contribution from each integration point to the Jacobian used in the iterative solution for that equilibrium is given by the inverse of the elasto-plastic compliance: the Jacobian in equation (2.6). That is taken to relate the deformation rate to the Jaumann stress rate, and the stress is taken to rotate with the material, *not* the crystal, reference frame. All the iterations described above need to be damped. The iteration, equation (2.6), is carried out at constant orientation: the orientation, and so the orientation-dependent Schmid matrix, is updated with each

successive refinement of equilibrium rather than within the stress iteration. Attempting to include orientation in equation (2.6) can lead to very unstable behaviour because the active systems can change quite abruptly. The incremental change in crystal orientation, $\Delta \boldsymbol{r}$, is given by the difference in overall rigid body rotation and that due to lattice spin,

$$\Delta r_{ij} = \Omega_{ij}\Delta t - \tfrac{1}{2}\{b_i n_j - b_j n_i\}_\alpha \Delta\gamma_\alpha, \tag{2.10}$$

where Ω is the rigid body spin of the overall deformation. In practice, $\Delta \boldsymbol{r}$ is translated into a change in the Euler angles of the crystal orientation.

With a rate sensitivity index of 0.01 or 0.02, overall deformation increments of about 0.002–0.005 can be used, and convergence of all the iterations to reasonable accuracy (10^{-4}) *usually* occurs in only a few steps. Exceptions occur when slip-system changes take place, but poor convergence due to this has not propagated beyond the first stages of load equilibrium iteration. Despite generally well-behaved algorithms, the number of calculations involved is considerable, and even with fairly simple problems the computation time is large. For that reason, all the examples given below are two dimensional, i.e. plane strain, and use only a few hundred eight-node quadrilateral or six-node triangular elements.

3. Examples

As far as material behaviour is concerned, the form and evolution of the orientation and the slip resistances, $\boldsymbol{\tau}^0$ are of primary interest. It is of course possible to investigate the effect of different types of slip systems, but in this work octahedral slip typical of FCC metals is used, with a small rate sensitivity. The small, instantaneous, slip-rate sensitivity is really a mathematical convenience to avoid the 'on-off' discontinuity in slip-system activity of the Bishop and Hill analysis, although it does correspond to the type of value observed experimentally with abrupt changes in loading rate.

The material state at any point is determined by the Euler angle set describing the orientation and the $\boldsymbol{\tau}^0$. For $\{111\}\langle 110\rangle$ slip this gives an *apparent* number of 15 state variables. The evolution of the Euler angles follows from equation (2.10). The evolution of $\boldsymbol{\tau}^0$ and the interpretation of this aspect of the material state is potentially a significant factor in attempting to model the development of structure by the CPFEM. The simplest useful model is one where the $\boldsymbol{\tau}^0$ are all equal at any point in space and time: 'isotropic' hardening. Some interesting results can be obtained even with this approximation, and some examples are given below before dealing, finally, with the possibility of going beyond that approximation.

(a) *Deformation zones at inclusions*

Humphreys and his co-workers have carried out much work on recrystallization nuclei forming at the deformation zones surrounding inclusions. One particular case was the occurrence of 'plumes' at silicon particles in aluminium crystals of initial orientation (001) [110], deformed in plane-strain compression (Humphreys & Ardakani 1994). Crystal rotations carried the bulk of the material towards one variant of the 'copper' orientation, near $\{112\}\langle 111\rangle$, whereas the 'plume' orientations were of the mirror-symmetry-equivalent 'copper' orientation. Results using the model described

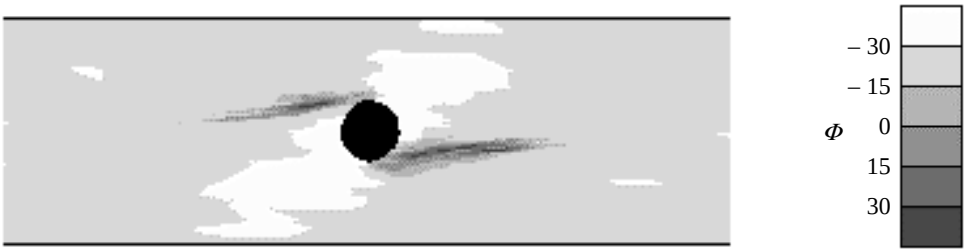

Figure 1. Contours of Euler angle Φ in the 'matrix' surrounding an elastic inclusion. Plane strain, $\varepsilon_{xx} = 1$. The start orientation was perturbed 3° away from ideal (001) [110], and most of the matrix has rotated towards the 'copper' orientation. Note the 'plumes' that have rotated towards the complementary 'copper' orientation.

above are given in figure 1. The plumes are predicted reasonably well in this case, and this is a relatively straightforward application.

The hardening rule used was of the Voce type,

$$\tau_\alpha^{0+} = \tau_\mathrm{s} - (\tau_\mathrm{s} - \tau_\alpha^0) \exp\left(-\eta \sum |\Delta\gamma_\beta|\right), \tag{3.1}$$

where the saturation stress, τ_s, was set to have a rate invariant value of 50 MPa, η was 3.5 and the initial values of $\boldsymbol{\tau}^0$ were 20 MPa. This type of hardening rule actually only requires one state variable in addition to the orientation triplet. More complex isotropic hardening models would require perhaps only two or three to give very accurate representations of overall stress–strain response in proportional loading.

(*b*) *Relaxed constraint effects on texture*

Rather than having an elastic inclusion, we can consider a plastic inclusion: a grain surrounded by grains of different orientations. Although most models of texture development involve very simple rules about how a grain would deform within a polycrystal, details of the interaction of a grain with its neighbours are very significant, as shown by the work by Sarma & Dawson (1996*b*). Unfortunately, such analyses become very computationally demanding in realistic cases, involving a statistically significant number of grains and three spatial dimensions.

An interesting simple case is that of an embedded 'cube' grain with an overall deformation consisting of plane strain with a simple shear component. This is the type of deformation found away from the mid-plane of plate during rolling, and of course the stability of 'cube' grains is important because they become nuclei for subsequent recrystallization. The 'cube' orientation actually has a high resistance to the simple shear, which aids its stability particularly when the original grain has become flattened. This flattening leads to the possibility of geometric relaxation of constraint (Honeff & Mecking 1978), and figure 2 shows results for a 'cube' grain embedded in a matrix of six other grains of randomly selected orientations, deformed with a simple shear rate one-third of the plane-strain rate imposed at the boundary. During early stages of deformation, moderately large orientation gradients, relative to the overall strain, are set up in the 'cube' grain, but with increased straining these actually decrease to some extent, demonstrating the geometric relaxed constraint effect. This

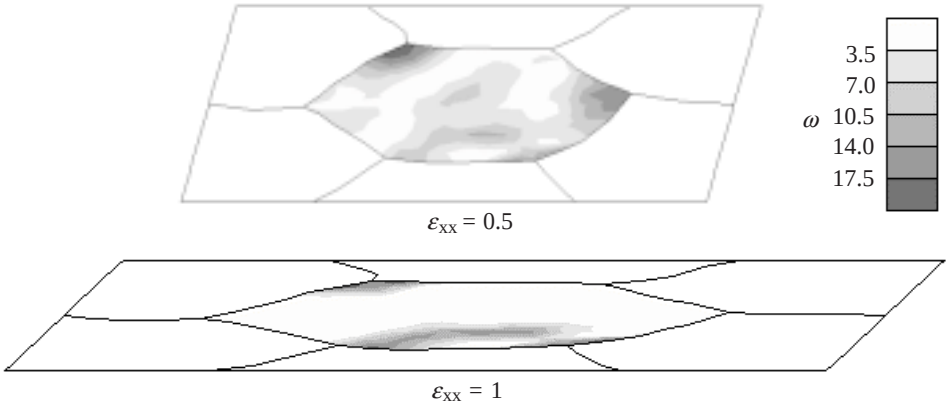

Figure 2. Misorientation, in degrees relative to 'cube', in an initially 'cube' grain embedded in six random grains subject to a combination of plane strain and simple shear at the boundary. The misorientation decreases with increasing strain as the grain becomes flattened. The 'full constraint' Taylor model predicts uniform misorientations of 5° at $\varepsilon_{xx} = 0.5$ and 10° at $\varepsilon_{xx} = 1$.

of course also means greater shearing and inhomogeneity in the surrounding grains, into which subgrains from the 'cube' grain will grow.

Although of no great importance to the results, this example used the Voce-type model, equation (3.1), with a rate-sensitive saturation stress,

$$\tau_{\mathrm{s}} = C\left(\sum |\dot{\gamma}_\beta|\right)^n, \tag{3.2}$$

with a value for C of 56 MPa and a value for the rate sensitivity of saturation stress, n, of 0.02.

(c) *Orientation splitting*

Figure 2 also shows the development of a local band of relatively high misorientation within the 'cube' grain. This type of feature occurs very often, with many other initial orientations, in this type of multi-crystalline simulation as a result of intergranular effects. There are cases where orientation banding is predicted to occur in 'single' crystals, with 'isotropic' hardening. An example of this is shown in figure 3, where an initial orientation near $(332)\,[\bar{1}\bar{1}3]$ is subject to ideal plane strain at the domain boundary. This orientation would rotate towards 'Goss' according to the simple Taylor model, whereas the CPFEM predicts that it splits into alternate bands which rotate towards either 'Goss' or the 'copper' orientation. The mechanical advantage gained from this behaviour is that, in early stages of deformation, complementary simple shears are associated with the bands. The case shown started out 5° away from the 'watershed' predicted by the Taylor full constraint (FC) model, and some material is predicted to rotate towards 'copper' with start orientations somewhat further away from that point. This type of behaviour naturally applies to a whole range of other orientations.

(d) *Bicrystal simulation*

A major incentive for the prediction of deformation microstructure, after large deformations anyway, is that the recrystallization behaviour depends critically on

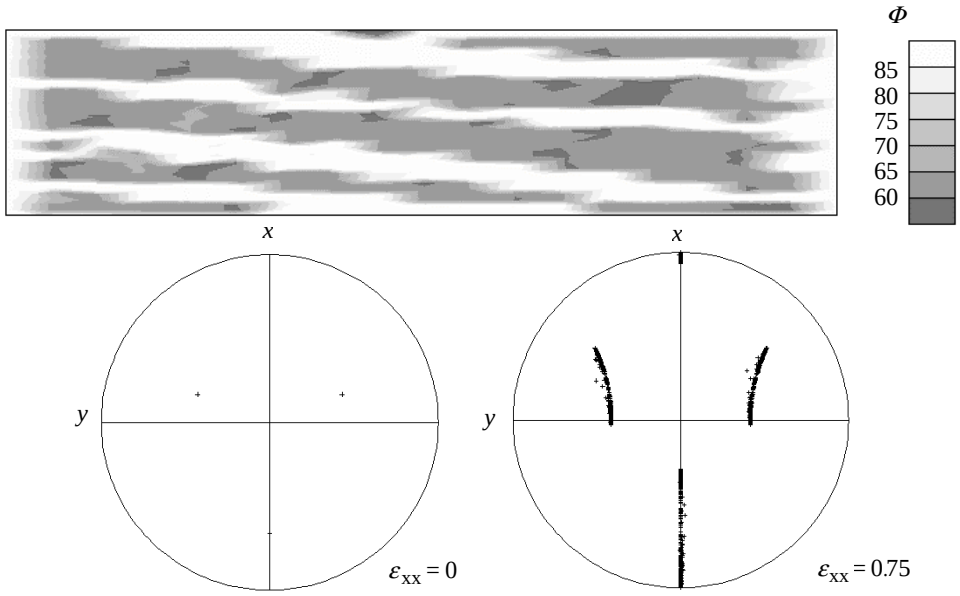

Figure 3. Simulation of plane-strain compression, to a strain of $\varepsilon_{xx} = 0.75$, of a region with an initial orientation $\langle \varphi_1, \Phi, \varphi_2 \rangle = \langle 90°, 67°, 45° \rangle$. The orientation splitting is shown as 001 'pole figures'.

that microstructure. It is known that prior grain boundaries are common sites for the nucleation of recrystallization. One reason for this is, naturally, the availability of a mobile high-angle boundary, but the difference in mechanical response due to the initial orientation difference is also important. Usually, it is assumed that a greater amount of deformation occurs adjacent to the boundary, but in fact there is a large range of orientation pairing where mutual relaxation of constraint can mean that the boundary region is effectively 'softer'. A somewhat artificial example showing this is the 'full constraint' deformation of a bicrystal, the two orientations of which would shear in opposite ways under 'relaxed constraint' conditions. Such an example, with no special choice of initial orientations, is shown in figure 4.

Various features are apparent. The orientations develop, with considerable spread, towards complementary 'S' orientations. Deformation banding develops, giving a 'herring bone' pattern, most obvious in the plastic strain distribution, figure 4*a*, but also noticeable in the spatial variation of crystal orientation, figure 4*c*. There is a large orientation gradient adjacent to the boundary within one of the grains, and there is a coincident gradient in the von Mises effective stress, figure 4*b*, with low stresses near the boundary.

Now, the von Mises stress might seem to be irrelevant, or even obsolete, in the context of slip-based modelling. However, it is likely to provide a reasonably good measure of the overall resistance to deformation and so the density of substructure formed. In this example, all the slip resistances have essentially reached saturation level (equation (3.1) was used), but that does not take into account the orientation-related overall resistance. The von Mises stress includes the 'Taylor factor'-type

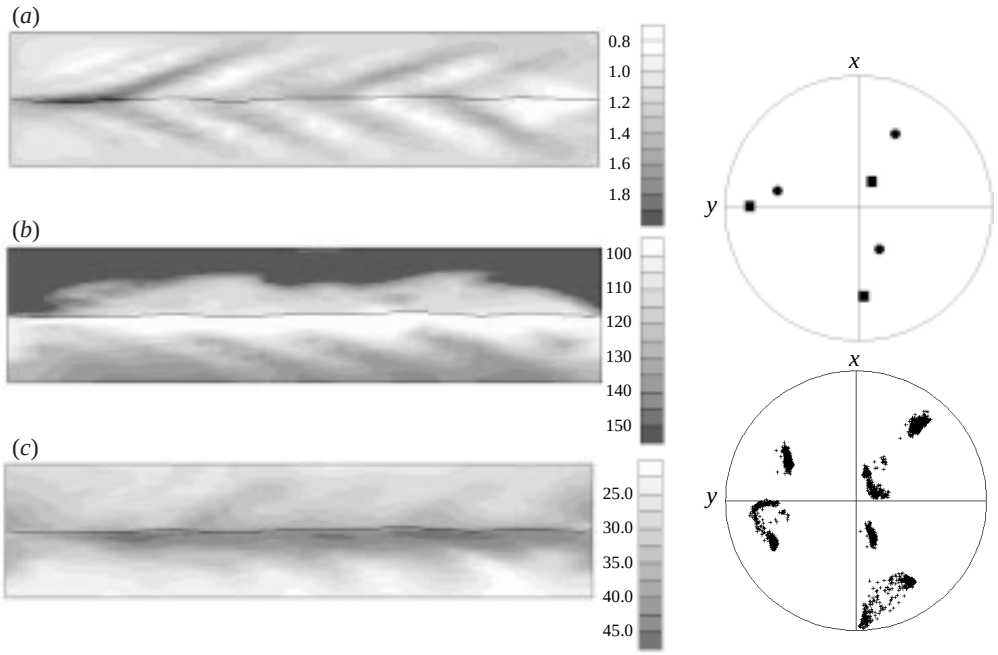

Figure 4. The predicted state of a bicrystal deformed in plane strain to $\varepsilon_{xx} = 1$. Deformation banding is apparent, as is the reduction in effective stress and the development of orientation gradients at the boundary. The initial orientations and final orientations of integration points are shown as 001 'pole figures' on the right.

effects and it seems reasonable that substructural density would depend on that as well as slip resistance.

If the assumption is made that the final von Mises stress is linearly related to the substructure density in metals which undergo extensive dynamic recovery to give a cell or subgrain structure, then the output from the CPFEM simulation can be used as input to a two-dimensional 'network' model for recrystallization (Humphreys 1993). Cell centres were included at random coordinates within the domain, with exclusion conditions to ensure that the separations were inversely proportional to the local von Mises stress. Cell orientations were directly interpolated and the initial network set up via a Dirichlet tessellation. Two stages in the development of such an annealing simulation is shown in figure 5.

At the early stages of 'annealing', the essential features of the deformed structure are apparent. The crystallite size is larger, and there are more high-angle boundaries, near the original grain boundary. There are some moderately high-angle boundaries associated with the deformation inhomogeneity in the upper grain. At the later stage shown, considerable 'strain-induced boundary migration' has occurred, with two groups of recrystallized grains. These have orientations corresponding to a 'cube' texture rotated by 15° about the extension direction.

The growth of the near-'cube' grains depended critically on the model describing the energy and mobility of the boundaries. Simply having reduced mobility and energy of low-angle boundaries allowed growth of one 'S' component into the other, and it was necessary to reduce the mobility of high misorientations, close to $\Sigma 3$, as

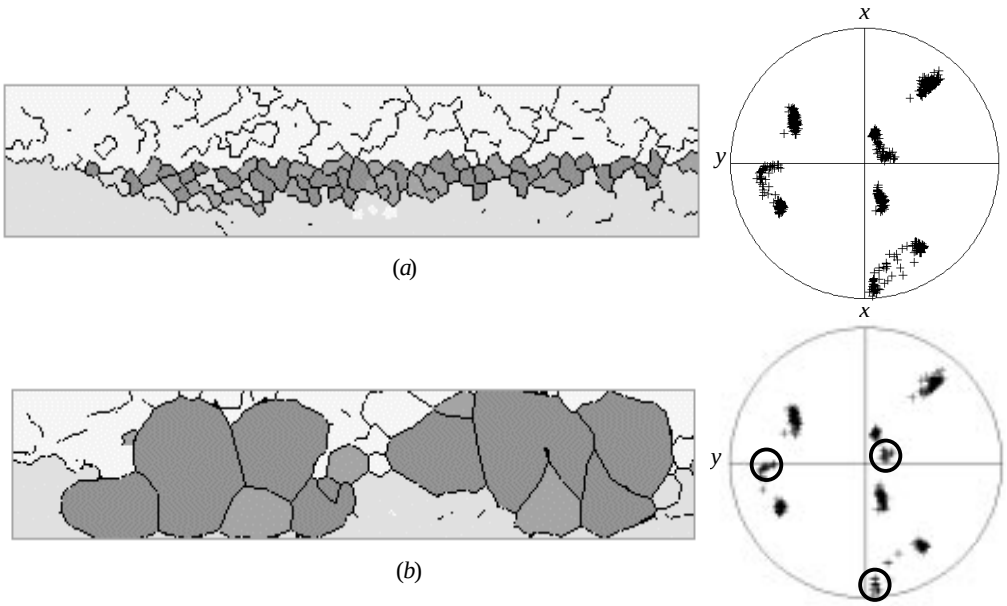

Figure 5. Results from a 'network' annealing model with the initial representation of microstructure derived from the CPFEM results shown in figure 4. The initial number of crystallites was 900, as shown in (*a*). Only boundaries with misorientations greater than 3° are shown, and darker grains are near $\{001\}\langle 100\rangle$. The configuration at 400 crystallites is shown in (*b*); the 'recrystallizing grain' orientations are circled in the 001 'pole figure' shown to the right.

well. It is clear that detailed knowledge of the variation of boundary properties with misorientation, and possibly inclination, will be needed for this type of modelling to be useful, irrespective of the accuracy with which the CPFEM can predict the deformed structure.

(*e*) *Deformation banding*

The last example showed some evidence of deformation banding, and the prediction of such a common feature in deformed microstructures would be of considerable value. Banding features are readily seen in the simulations of plane-strain compression of the 'copper' orientation, such as that shown in figure 6.

There are a few interesting aspects of these bands. The inclination of the 'strain' bands (30°) is less than that of the 'orientation' bands (40°). This is not simply because the 'strain' bands represent the accumulation of deformation, and so are subject to a rigid-body rotation. In fact, the effective strain rate is inhomogeneous in bands inclined at *ca.* 35°. Neither of the major band types has an obvious crystallographic origin, although the low inclination 'sub-banding' might.

The mean stable orientation is near $\Phi = 30°$, which is close to that observed in real deformation textures of polycrystals. This is intermediate between the Taylor FC ($\Phi = 27.4°$) and RC ($\Phi = 35.3°$) predictions, and the apparent reason for the banding is that the 'material' is achieving a degree of relaxation of constraint by inhomogeneous deformation. Many orientations will then undergo similar 'relaxed

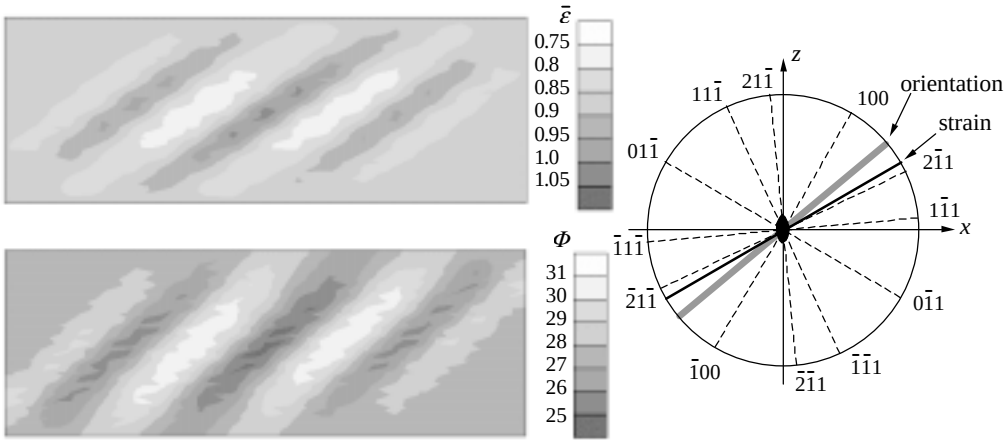

Figure 6. Plane-strain compression, with 'full constraint' boundary conditions, of the 'copper' orientation to $\varepsilon_{xx} = 0.75$. Effective strain levels are shown above contours of the Euler angle, Φ, in degrees. Bands are seen in each case, the orientations with respect to crystal directions in the plane are shown to the right.

constraint' banding, but predictions of this behaviour are limited here by the plane-strain assumptions.

Reasons for the formation of deformation bands have been listed by Dillamore *et al*. (1972). The banding predicted in the examples shown in figures 3 and 6 is essentially due to the third of those reasons—reduction in overall work by inhomogeneous deformation—and it is likely that the CPFEM will deal with all but one of their list. That exception is related to the possibility of different sets of systems achieving the same strain rate but different rotations. Although relaxation of constraint will avoid that indeterminacy, it is difficult to see how the CPFEM can deal with that possibility in all cases. The question arises as to how a selection between mechanically equivalent sets could arise. Although there are various mathematical techniques for avoiding indeterminacy of slip-system selection, it seems likely that the material solves it by orientation splitting at the level of the deformation substructure and grains split into regions in which a subset of the 'Taylor' systems are operative.

In the continuum approach, there needs to be some mechanical advantage for such orientation splitting, and this must then be a feature of the constitutive model. One possibility is that 'latent hardening'—the hardening of 'inactive' systems relative to 'active' ones—could lead, locally, to a minimization of the number of slip systems and so to more accurate simulation of orientation splitting.

It is well known that simply adding up the amount of slip and taking that sum to determine hardening is a fairly poor approximation. Crystals deforming by single slip show much lower hardening rates than those deforming by multiple slip, and there is much evidence that dislocation accumulation leads to oriented structures which give anisotropic hardening, so that typically systems that are not active give higher slip resistances than those in which slip is occurring to a significant extent. A simple way of implementing latent hardening, which is satisfactory for the purposes of showing the type of effect that such 'anisotropic' hardening will have, is to use the Voce-type model but make the saturation slip resistance different on different systems. To do

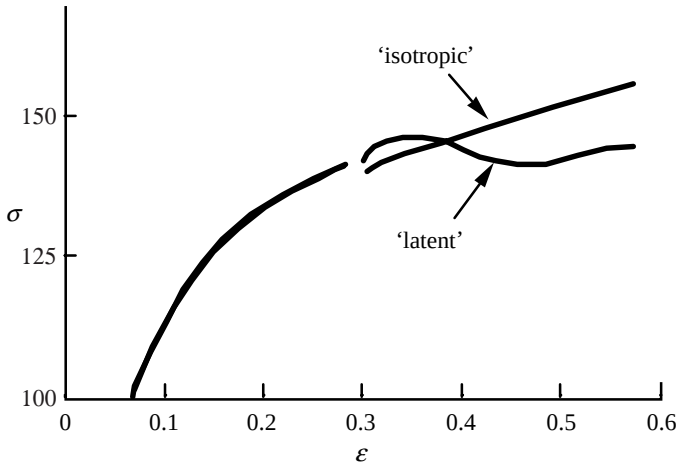

Figure 7. The (effective) stress–strain curves for 'copper' orientation prestrained in plane strain and then subject to shear, with both 'isotropic' and 'latent hardening' ($B/A = 0.43$).

this, equation (3.1) is modified so that

$$\tau_\alpha^{0+} = \tau_\mathrm{s}^\alpha - (\tau_\mathrm{s}^\alpha - \tau_\alpha^0) \exp\left(-\eta \sum |\Delta\gamma_\beta|\right), \tag{3.3}$$

where the individual saturation stresses are determined by a weighted sum of the absolute slip rates:

$$\tau_\mathrm{s}^\alpha = A + B \frac{\sum S_{\alpha\rho} |\dot{\gamma}_\rho|}{\sum |\dot{\gamma}_\rho|}. \tag{3.4}$$

The matrix $\boldsymbol{S}$ describes the latent hardening effect, B the overall magnitude and A the 'isotropic' component. All elements of $\boldsymbol{S}$ are positive—maximum unity—and zero if a diagonal element. Slip on a single system then gives the saturation stress on that system equal to A, but for other systems it will be higher, up to a maximum of $A + B$. There are many possibilities for the exact form of $\boldsymbol{S}$, but here only the extreme case of penalization is considered. This means that

$$S_{\alpha\beta} = 1 - \delta_{\alpha\beta}. \tag{3.5}$$

The effect of this on the mechanical response of a 'copper'-oriented region subject first to plane strain and then to a (negative) shear to give an orthogonal change in strain path direction is shown in figure 7.

Now, although the mechanical response to changes in straining state predicted using this approach are, very approximately, of the correct form, the effect on deformation banding is relatively minor. Orientations for which no deformation banding is predicted using the (two-dimensional) isotropic model do not show banding with latent hardening, including other forms to the one used above, equation (3.5). The effect of latent hardening on the prediction of banding in the 'copper' orientation is shown in figure 8.

Clearly, there is no major effect. There is a slight increase in the degree of inhomogeneity, but the angles of the bands are the same as those predicted with 'isotropic' hardening. It appears that 'latent' hardening, at least with the simple formalism used here, does not encourage the local selection of slip system subsets to any greater

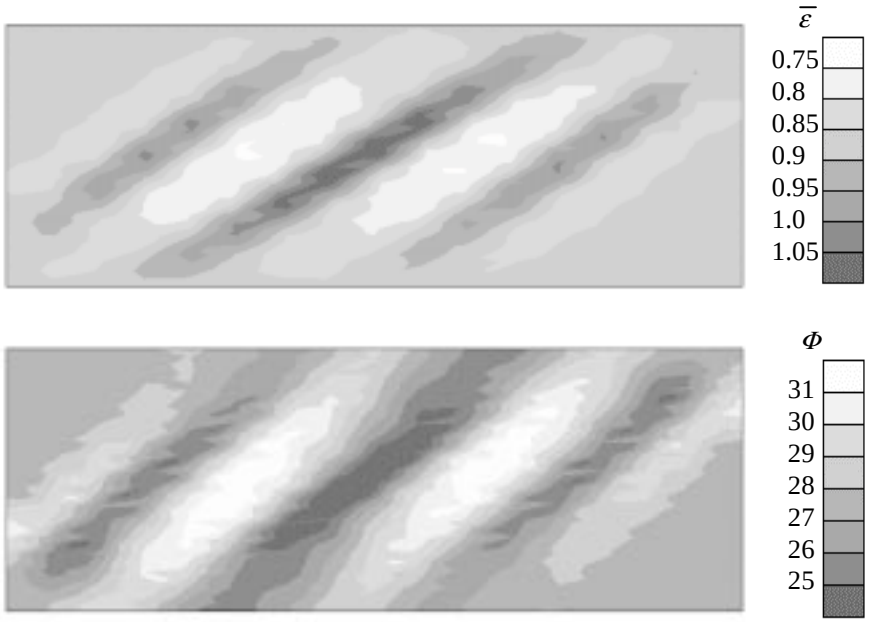

Figure 8. Plane-strain compression, with 'full constraint' boundary conditions, of the 'copper' orientation to $\varepsilon_{xx} = 0.75$ with 'latent' hardening ($B/A = 0.25$). The quantities and levels are as in figure 6.

degree than does 'isotropic' hardening. It may even be that the CPFEM is inherently incapable of predicting the substructure-scale effects observed in reality and that the limits of the continuum approach have been reached.

4. Summary

There is in principle a great deal of freedom in the CPFEM to take into account the real effects of dislocation interactions and accumulation. However, at some stage the limits of the 'continuum' plasticity assumptions will be met and further details of the nature of the deformation microstructure inferred from state variables involved in a constitutive model. It is fairly obvious that constitutive models used in finite-element modelling do not have a length-scale: for example, it is difficult to see how the Hall–Petch relationship could be predicted from polycrystal models of the type dealt with above. It is possible to construct plasticity models which contain a dependence of flow stress on gradients of plastic strain (Aifantis 1986), and for the continuum modelling of microstructure this type of approach may be useful. However, FE models with high-order field continuity would be required for their application and this poses a significant difficulty.

Despite this limitation, the CPFEM does give potentially useful simulations of some aspects of deformation microstructure. Its value in the field of deformation textures and inhomogeneous intragranular deformation is well established and even simple interpretations of state, such as the correlation of effective stress with sub-boundary density, should allow the prediction of some recrystallization nucleation

events. If that is indeed the case, then the method will have a valuable role in an important and difficult area of materials engineering.

The author would not have engaged in this activity without the encouragement of F. J. Humphreys and W. B. Hutchinson, and thanks them for that, and S. J. Lillywhite for constructive criticism of the manuscript. The work has been supported by the Engineering and Physical Sciences Research Council (GR/L65857) and Alcan International.

References

Aifantis, E. C. 1986 On the dynamic origin of dislocation patterns. *Mater. Sci. Eng.* **81**, 563–574.

Dawson, P. R. & Marin, E. B. 1997 Computational mechanics for metal deformation processes using polycrystal plasticity. *Adv. Appl. Mech.* **34**, 77–167.

Dillamore, I. L., Morris, P. L., Smith, C. J. E. & Hutchinson, W. B. 1972 Transition bands and recrystallization in metals. *Proc. R. Soc. Lond.* A **329**, 405–420.

Eshelby, J. D. 1958 Scope and limitations of the continuum approach. In *Internal stresses and fatigue in metals* (ed. G. M. Rassweiler & W. L. Grube), pp. 41–58. Amsterdam: Elsevier.

Honeff, H. & Mecking, H. 1978 A method for the determination of the active slip systems and orientation changes during single crystal deformation. In *Textures of Materials, 5th ICOTOM* (ed. G. Gottstein & K. Lücke), pp. 265–275. Berlin: Springer.

Humphreys, F. J. 1993 A microstructural model of recrystallisation. *Mater. Sci. Forum* **113–115**, 329–334.

Humphreys, F. J. & Ardakani, M. G. 1994 The deformation of particle-containing aluminium single crystals. *Acta Metall. Mater.* **42**, 749–761.

Kalidindi, S. R., Bronkhorst, C. A. & Anand, L. 1992 Crystallographic texture evolution in bulk deformation processing of FCC metals. *J. Mech. Phys. Sol.* **40**, 537–569.

Peirce, D., Asaro, R. J. & Needleman, A. 1982 An analysis of non-uniform and localised deformation in ductile single crystals. *Acta Metall.* **30**, 1087–1119.

Peirce, D., Asaro, R. J. & Needleman, A. 1983 Material rate dependence and localised deformation in crystalline solids. *Acta Metall.* **31**, 1951–1976.

Sarma, G. B. & Dawson, P. R. 1996*a* Effects of interactions among crystals on the inhomogeneous deformation of polycrystals. *Acta Mater.* **44**, 1937–1953.

Sarma, G. B. & Dawson, P. R. 1996*b* Texture predictions using a polycrystal plasticity model including neighbor interactions. *Int. J. Plasticity* **12**, 1023–1054.

van der Giessen, E. & Needleman, A. 1995 Discrete dislocation plasticity—a simple planar model. *Modelling Simul. Mater. Sci. Engng* **3**, 689–735.

PHILOSOPHICAL TRANSACTIONS OF THE ROYAL SOCIETY A MATHEMATICAL, PHYSICAL & ENGINEERING SCIENCES